IJAME

Int. J. of Applied Mechanics and Engineering, 2025, vol.30, No.4, pp.125-136
DOI: 10.59441/ijame/208784

ANALYSIS OF BIONIC RIBLET STRUCTURES INFLUENCE ON CENTRIFUGAL PUMP PERFORMANCE

R.J. Pawar*, M.P. Ray, S.R. Suryawanshi and D.K. Dond
Department of Mechanical Engineering, MET BKC Institute of Engineering, Nashik, SPPU Pune, INDIA
E-mail: pawarraj7938@gmail.com

The growing need for energy conservation and sustainability in industrial sectors has led to extensive research on improving mechanical systems, particularly centrifugal pumps. These pumps play a crucial role in hydropower generation, industrial processes, and fluid transportation. This study explores the use of biomimetic riblet structures inspired by shark skin to enhance centrifugal pump performance. Traditional designs focus on either hydraulic efficiency or noise reduction, leaving room for improvement. By developing and experimentally testing a bionic impeller, the research examines its impact on head, power consumption, and efficiency across different flow rates. While biomimetic adaptations are common in aerospace and marine engineering, their potential in pumps remains underexplored. Comparative analysis evaluates the effectiveness of these modifications in optimizing performance. Experimental findings provide insights into improved fluid movement and energy efficiency. By integrating nature-inspired design with testing, this research explores the performance enhancement of fluid transportation systems through the use of a bionic impeller. The technology demonstrates an efficiency gain of up to *3.2%* at a discharge rate of *12 m³/h*, with improvements reaching around *8%* at higher flow rates. The bionic impeller effectively reduces turbulence, optimizing pump efficiency and leading to energy savings, reduced operational costs, and improved sustainability in industrial fluid transport systems.

Key words: bionic impeller, centrifugal pump, biomimetic riblet structure, shark skin.

1. Introduction

The world is facing two big problems: energy scarcity and environmental degradation. These issues make it more important than ever to improve energy efficiency in industries [1, 2]. One area where significant improvements can be made is in the operation of centrifugal pumps. These pumps are widely used in hydropower stations and many industrial processes [3]. They play a key role in moving fluids, but they also consume a lot of energy. This means even small improvements in their efficiency can lead to big energy saving [4, 5]. Centrifugal pumps are popular because they are cost-effective and flexible in how they can be used. However, most of their current designs focus only on either hydraulic performance (how well the pump moves fluid) or acoustic performance (how much noise the pump makes) [6]. These two factors are usually treated as separate concerns, and there is little effort to optimize them together. This leaves room for improvement.

One exciting area of innovation is biomimetic engineering-designing systems inspired by nature. In particular, scientists have looked at how shark skin reduces drag in water. Shark skin has tiny, ribbed structures called riblets that help the shark move through water more easily by reducing resistance [7]. Bio-inspired surface textures derived from shark skin morphology demonstrate exceptional drag reduction capabilities across engineering applications. Hybrid riblets achieve *34.5%* drag reduction on airfoils [8], while shark denticles provide *31%* reduction in fluid dynamic applications [9]. Convergent-divergent configurations reduce drag by *15%* on bluff bodies by altering vortex shedding [10]. Advanced manufacturing techniques, including optimized grinding, have improved fabrication quality and surface integrity [11]. Geometric analysis between natural and synthetic designs has refined engineered surfaces [12], with novel configurations achieving *21.45%* friction reduction in turbulent flows [13]. Marine vessel applications show enhanced speed

* To whom correspondence should be addressed

and efficiency through reduced hydrodynamic resistance [14]. Recent innovations in 3D-printed denticles with hydrophobic properties further optimize performance through controlled vortex formation [15].

This idea has already been applied successfully in other areas, like aircraft and ship designs, to improve efficiency. But there has been limited research on how these shark skin-inspired riblets could improve both the hydraulic and acoustic performance of centrifugal pumps [16].

This study focuses on applying shark skin-inspired riblet structures to the impellers of centrifugal pumps. By adding these riblet structures to the impeller, the goal is to see how they affect important performance measures like the pump's head (the height the fluid can be lifted), power consumption, and overall efficiency [17]. This study seeks to bridge a critical research gap by enhancing the fluid transport efficiency of centrifugal pumps while simultaneously improving their operational efficiency and reducing noise levels [18, 20].

The novelty of this work is introduction of shark skin-inspired riblet structures on centrifugal pump impellers to enhance efficiency and reduce drag, a largely unexplored approach. Unlike conventional designs, it simultaneously optimizes hydraulic and overall performance through experimental validation. In this experiment, an electromagnetic flow meter is used instead of a conventional flow meter to achieve higher accuracy [21]. A pump performance curve graphically illustrates how a pump operates under various conditions, helping engineers and users choose the most appropriate pump [22]. The Bernoulli equation serves as a fundamental tool for calculating head in fluid systems, with applications spanning pumps, turbines, pipelines, and hydraulic networks [23-25]. The study demonstrates energy savings, improved fluid dynamics, and reduced noise. [26-28].It highlights how bionic structures enhance centrifugal pump performance by promoting flow uniformity, reducing wall shear, and minimizing pressure pulsations, leading to a more stable flow field and lower energy loss for sustainable industrial applications [29, 30].

2. Experimental data collection

2.1. Experimental test rig

The block diagram of the experimental test rig is presented in Fig.1 [18].The test rig for experiment consists of a three-phase AC motor ($3.5\ kW$, $2900\ rpm$) and a HAS $40\times25\times175$ centrifugal pump. HSA denotes a high-efficiency horizontal centrifugal pump, with a *40 mm* suction, *25 mm* discharge, and *175 mm* impeller diameter.The test setup has one centrifugal pump driven by a motor with bearings. Water is taken from a built-in reservoir, moves through a filter and a valve, and then enters the pump through an inlet valve. After being pressurized, the water flows out through a delivery pipe. It then passes through an electromagnetic flow meter and returns to the reservoir. The adjustable inlet and outlet valves allow the reading at different duty points [19].

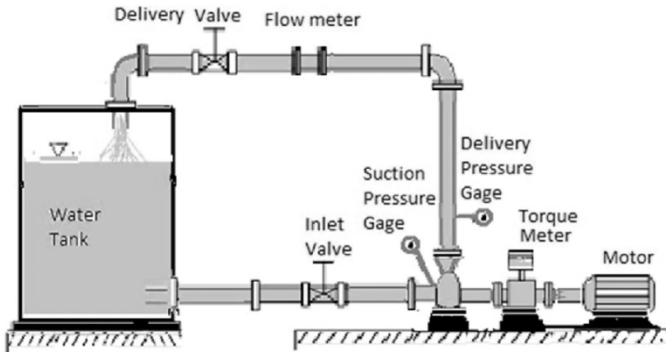

Fig.1. Experimental set up block diagram.

Instrument and control panel are located near pump test set up. The instruments display the pressure at inlet pressure, pressure at outlet and pressure difference. A variable frequency drive controls the pump at constant speed of *2900 rpm*.

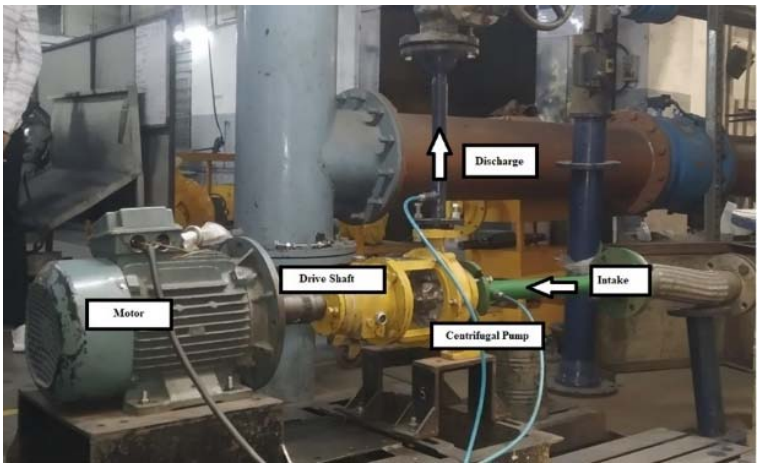

Fig.2. Actual pump model.

2.2. Collection of pump data

The pump set up is started and allowed to stable for some time till flow get stabilise. Once the flow has stabilized, a variable frequency drive is used to measure the impeller's revolutions per minute (RPM), the speed is first recorded. Then, the pressure head $\left(\text{in } kg/cm^2\right)$ is measured using a pressure gauge attached to the pump's discharge pipe. Input power is read and recorded from the pump test setup panels which consist of voltmeter, ammeter and gives power consumption in kilowatt [20].

2.3. Mesurement of discharge

Electromagnetic flow meters, are volumetric flow meters the operation of an electromagnetic flowmeter is based on induced voltage resulting from fluid passing through a magnetic field. This measurement is highly accurate for measuring fluids like water as they pass through a pipe because of no moving parts and no restriction in conduit [21]. The flow rate is varied by adjusting the discharge valve while maintaining a constant pump speed. Five duty points are selected based on the manufacturer's catalog and the IS: 13518.1992 standard. The selected flow rates $(0,\ 2,\ 5,\ 8,\ 12$ and $14\ m^3/h)$ cover various operational conditions, helping assess efficiency, power consumption, and head variations. These points align with manufacturer data and industry standards. The HSA $40\times25\times175.\ 10.049A$ pump follows standard naming conventions: HSA denotes a high-efficiency horizontal centrifugal pump, with a *40 mm* suction, *25 mm* discharge, and *175 mm* impeller diameter.

The Bernoulli equation, also known as the equation of energy, is utilized to calculate the total head H generated by a pump. Bernoulli's equation relates the pressure, velocity, and elevation at two points along a streamline. It is given by Eq.(2.1) [25]:

$$\frac{P_1}{\rho g}+\frac{V_1^2}{2g}+h_1=\frac{P_2}{\rho g}+\frac{V_2^2}{2g}+h_2+hf \tag{2.1}$$

where:

P – pressure at a point, N/m^2,

ρ – density of the fluid, kg/m^3,

g – acceleration due to gravity, $9.81\ m/s^2$,

V – velocity of fluid, m/s,

h – elevation or height above reference point, m,

h_f – head loss due to friction, m.

This equation represents the total head as the combination of head due to elevation, pressure head, velocity head, and the head losses that arise due to friction inside pipe (major losses) and flow disturbances caused by components such as bends and fittings (minor losses). In its simplified form, the Bernoulli equation often assumes that head losses are negligible [22].

2.4. Calculation of efficiency

Discharge $Q\ \left(m^3/s\right)$, measurements are conducted in six distinct sets, with each set comprising two replicates. The values from these replicates are averaged to determine the discharge for each set. Electromagnetic flow meters are employed for these measurements.
Considering negligible head loss (and correction factor, $\alpha = 0.13\ m$, head of the pump is given by Eq.(2.2) [23-25] as:

$$H = \frac{\Delta P}{\rho g} + \frac{V^2}{2g} + \Delta z, \tag{2.2}$$

H – total head,
ρ – water density $1000\ kg/m^3$,
ΔP – differential pressure, kg/cm^2,
Δz – elevation head, m,
$\frac{\Delta P}{\rho g}$ – pressure head, m,
g – gravitational acceleration $9.81\ m/s^2$,
$\frac{V^2}{2g}$ – velocity head, m.

The pump power to the water (output power) P_{output} , is computed as by Eq.(2.3) [24-25],

$$P_{output} = \rho g Q H \tag{2.3}$$

where: ρg – specific weight of water $9.81\ kN/m^3$.
The input power P_{input} supplied to the pump is recorded from the pump test rig control panel. The efficiency of pump is calculated as the ratio of output power to the input power as in the equation below [23-25].

$$\eta = \frac{P_{output}}{P_{input}} \times 100 \tag{2.4}$$

where, η pump efficiency in percentage.

3. Development of bionic structure

Bionic impellers are advanced devices designed by taking inspiration from nature to improve how fluids move through them. These impellers apply ideas from nature's designs to make them work more efficiently.

3.1. Shark skin inspiration

Shark skin has microscopic riblets (small longitudinal grooves) arranged in a specific pattern as shown in Fig.3 [26, 28]. These riblets help sharks swim efficiently by reducing drag and controlling flow separation.

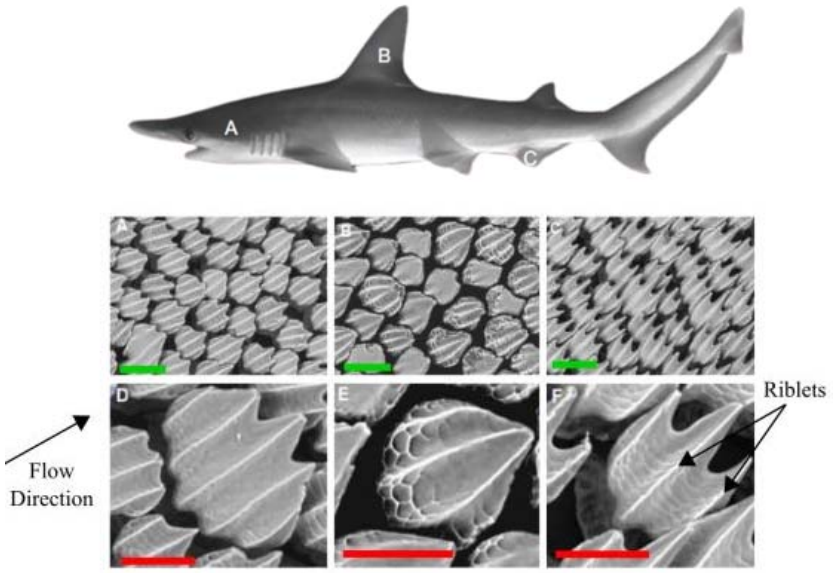

Fig.3. Riblets on shark skin at the head (A, D), dorsal fin (B, E), and anal fin (C, F), showing varied denticle structures. Flow direction: lower left to upper right. Scale bars: $200\mu m$ (green), $100\mu m$ (red).

3.2. Application to impeller

The spiral grooves visible on the impeller surface mimic this natural riblet structure. The grooves are precisely machined in a pattern that aligns with the anticipated fluid flow path. The dimensionless ratio of tooth distance to tooth height, a critical parameter, is maintained at *0.4*, as illustrated in Fig.4.

Fig.4. Bionic impeller.

Biomimetic riblet structures inspired by shark skin were applied to impeller blades to enhance performance. The triangular grooves, each *0.43 mm* high and with nine per vane (54 total), reduce drag and improve fluid flow. Oriented along the flow direction, the grooves minimize turbulence and energy loss, boosting efficiency and lowering energy consumption. Impeller blade geometry with biomimetic riblet placement is shown in Fig.5.

The manufacturing process of this semi closed impeller demonstrates the successful integration of modern CAD/CAM technology with traditional manufacturing methods. The combination of ArtCAM Pro software and CNC machining enables the production of complex fluid-flow geometries with high precision and repeatability. Figure 6 shows the ArtCAM tool path model.

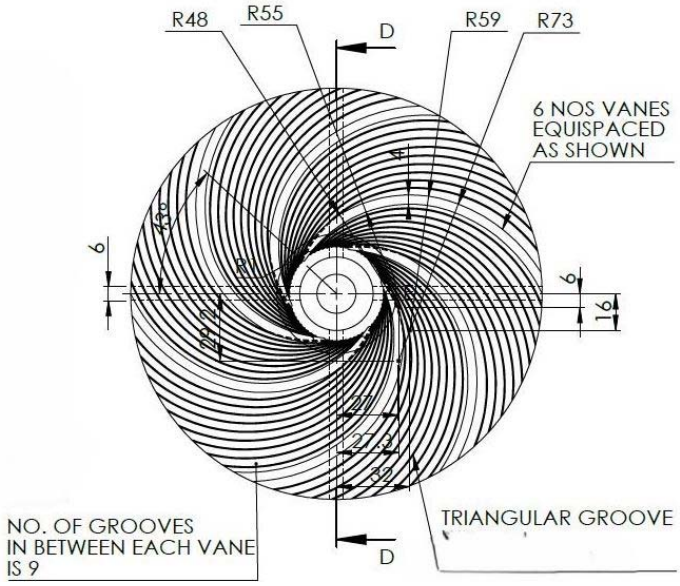

Fig.5. Impeller blade geometry with biomimetic riblet placement.

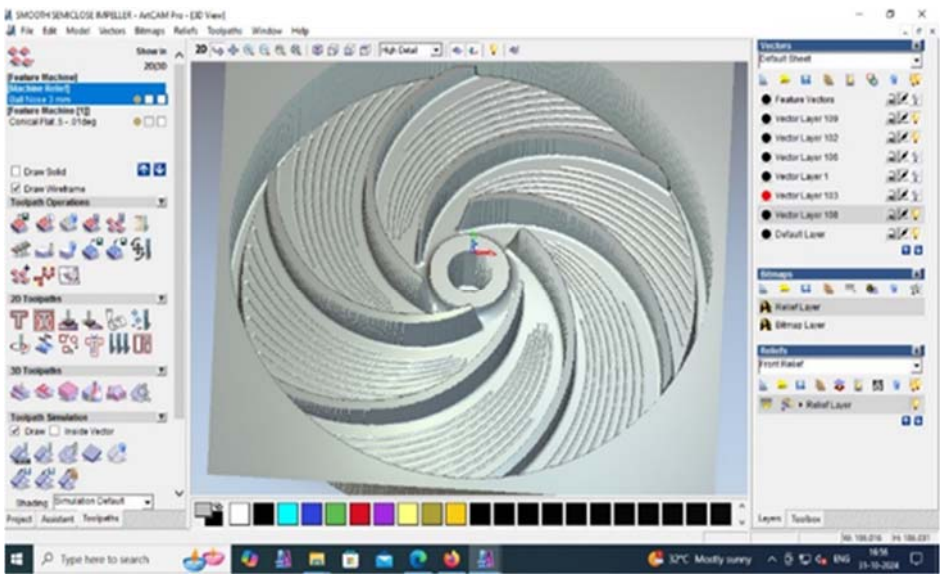

Fig.6. ArtCAM tool path model.

4. Pump performance analysis

The performance curves of a centrifugal pump are plotted by parameters such as head, flow rate, consumption of power, and efficiency curves. An increase in flow rate typically results in a reduction in total head, while power consumption rises due to higher hydraulic resistance [27]. Efficiency enhances with increasing flow, reaching its peak at the Best Efficiency Point (BEP), after which hydraulic losses become significant, leading to a decline in overall performance. Table 1 contains key performance parameters of a centrifugal pump with exsiting impeller at different operating conditions (duty points). The analysis of these parameters helps in understanding how the pump performs across various flow rates.

Table 1. Performance of pump using existing impeller.

Duty points	Units	1	2	3	4	5
Flow	$m^3/hr.$	*0*	*2*	*5*	*8*	*12*
Rotational speed	*RPM*	*2900*	*2900*	*2900*	*2900*	*2900*
Total head	*m*	*46.76*	*44.89*	*42.74*	*37.83*	*30.91*
Power	*kW*	*1.6*	*1.99*	*2.42*	*2.70*	*2.81*
Total efficiency	*%*	*0*	*12.28*	*24.07*	*30.53*	*35.99*

Table 2. Performance of pump using bionic impeller.

Duty points	Units	1	2	3	4	5
Flow	$m^3/hr.$	*0*	*2*	*5*	*8*	*12*
Rotational speed	*RPM*	*2900*	*2900*	*2900*	*2900*	*2900*
Total head	*m*	*47.36*	*45.58*	*43.26*	*38.64*	*32.75*
Power	*kW*	*1.55*	*1.84*	*2.27*	*2.55*	*2.73*
Total efficiency	*%*	*0*	*13.42*	*25.95*	*33.05*	*39.21*

Table 2 contains key performance parameters of a centrifugal pump with bionic impeller at different operating conditions (duty points).

The experimental comparison of the performance characteristics between an existing impeller design and a bionic impeller design highlights several critical differences across various discharge rates in Fig.7. The results provide valuable insights into the relative strengths and weaknesses of each design in terms of head (pressure), power consumption, and efficiency.

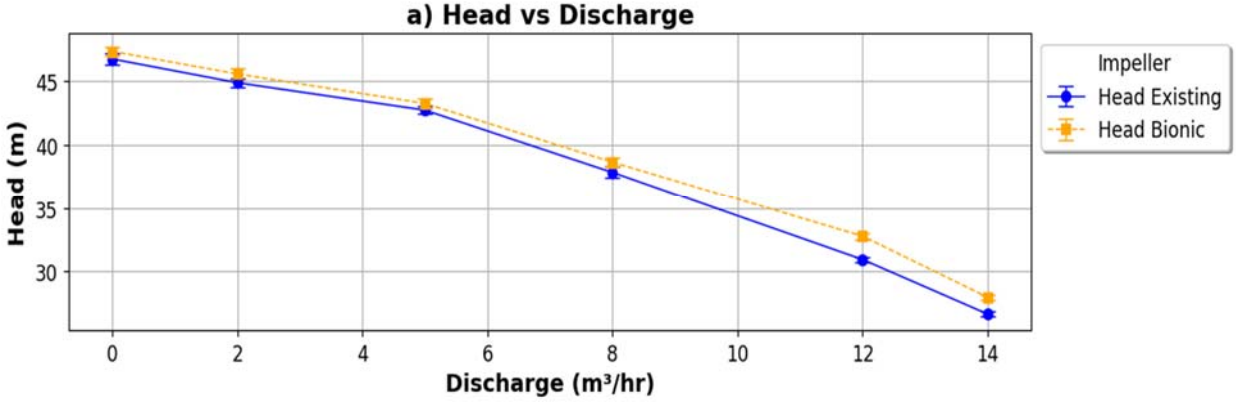

Fig.7. Performance test curve at different duty points for existing and bionic impeller: a) Head vs Discharge, b) Power vs Discharge, c) Efficiency vs Discharge.

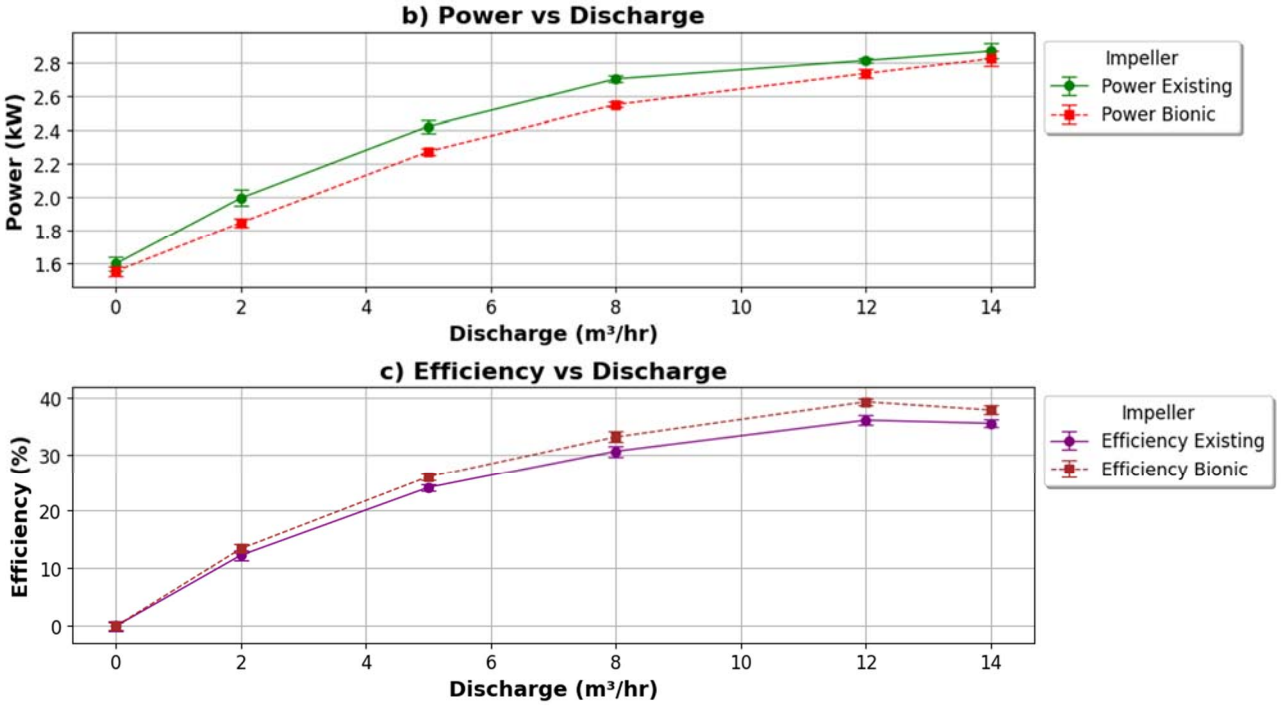

Fig.7 cont. Performance test curve at different duty points for existing and bionic impeller: a) Head vs Discharge, b) Power vs Discharge, c) Efficiency vs Discharge.

The comparative performance analysis of the bionic impeller and the conventional impeller demonstrates a notable advantage in terms of head generation, power consumption, and efficiency across all discharge rates.

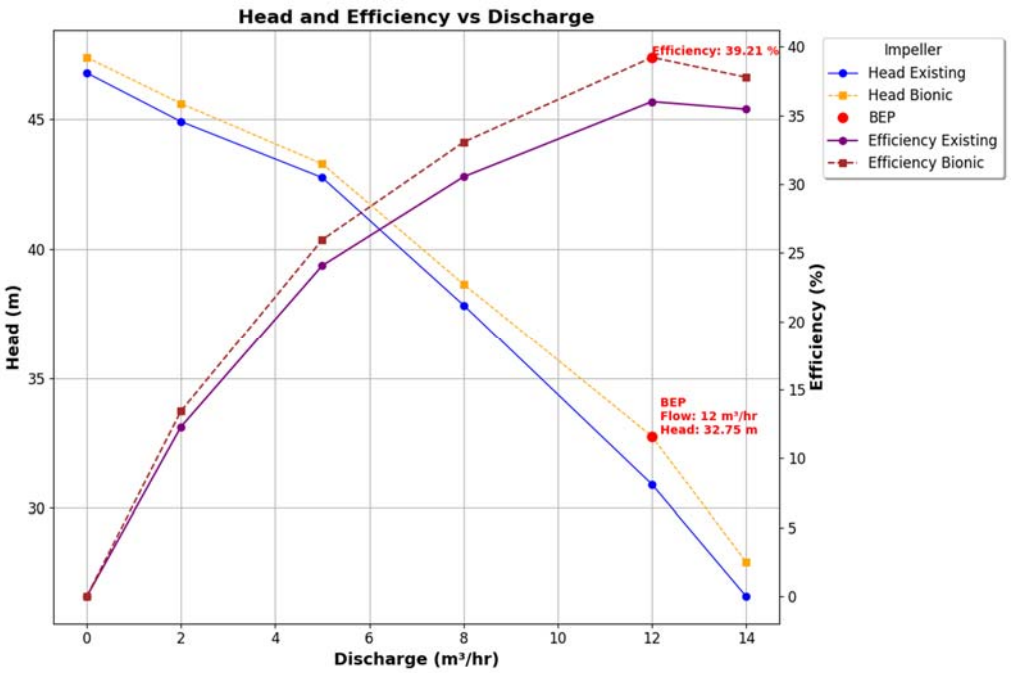

Fig.8. Performance test curve at different duty points for existing and bionic impeller with BEP.

The bionic impeller consistently maintains a higher head, indicating its enhanced capability to sustain superior pressure performance under identical operating conditions. Both impellers exhibit a linear decline in head with increasing discharge, a characteristic trend in centrifugal systems due to the inverse relationship between flow rate and pressure. However, the bionic impeller's design modifications enable improved pressure retention at higher flow rates. Additionally, the bionic impeller requires lower power input across all discharge levels, emphasizing its energy-efficient characteristics. Both impellers display a linear increase in power consumption with rising discharge, aligning with the expected correlation between flow rate and energy input in fluid systems. In terms of efficiency, the bionic impeller demonstrates superior performance throughout the discharge range, attributed to its optimized fluid dynamics and reduced energy losses. The efficiency advantage becomes more pronounced at higher discharge rates, further reinforcing the bionic impeller's suitability for high-flow applications where energy conservation and operational stability are critical considerations.

This Fig.8 presents a performance comparison between an existing impeller and a bionic impeller design, focusing on key metrics such as head, efficiency, and the Best Efficiency Point (BEP). The bionic impeller achieves a BEP at a discharge rate of *12 m^3 / hr* , with a head of *32.75 m* and an efficiency of *39.21%.*

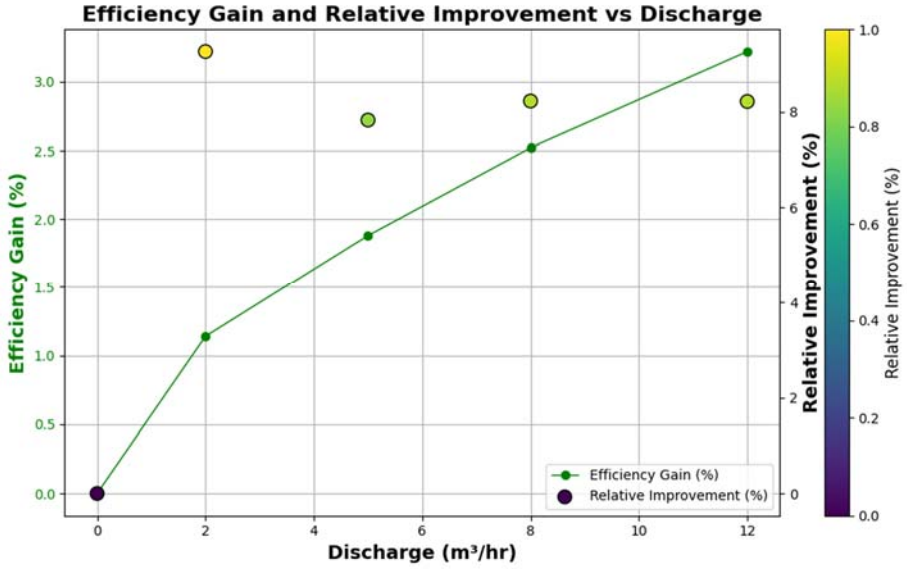

Fig.9. Efficiency gain and relative improvement across flow rates.

Figure 9 compares the performance of the bionic and existing impellers across different flow rates. The efficiency gain increases with discharge, reaching about *3.2%* at *12 m^3 / hr* . Relative improvement also rises, peaking around *8%* at higher flows. The bionic impeller shows the most significant benefits in high-flow conditions, suggesting its effectiveness in reducing turbulence and improving pump efficiency. Across the discharge range, the bionic impeller consistently maintains a higher head and demonstrates superior efficiency, particularly at higher discharge rates. These findings highlight the bionic impeller's potential advantages in high-flow applications, offering improved pressure performance and energy efficiency compared to the existing design.

5. Conclusion

This paper investigates a bionic impeller by experimenting with an existing impeller used in a centrifugal pump under a proven setup. The conclusions have been made based on the experimental results.

1) The bionic impeller enhances centrifugal pump performance by achieving higher head and better pressure retention across all discharge rates.

2) The bionic impeller reduces power consumption, offering an energy-efficient and sustainable design with lower hydraulic losses.
3) The bionic impeller achieves superior efficiency, especially at higher flow rates, due to enhanced fluid dynamics.
4) The performance curves show a linear head decline and power increase with discharge, aligning with typical centrifugal pump behavior.
5) The bionic impeller reaches its Best Efficiency Point at $12\ m^3/hr$ with 39.21% efficiency, outperforming the conventional impeller for high-flow applications.
6) The findings confirm that biomimetic riblet structures enhance pump efficiency, leading to energy savings and greater operational stability.
7) Bionic principles in pump design offer a promising path to optimizing performance and advancing sustainable, high-efficiency centrifugal pumps.

The bionic impeller offers multiple opportunities for advancement, including using durable, corrosion-resistant materials for harsher environments and customizing it for various fluid types. Additionally, it could enhance renewable energy applications and be adapted for different pump configurations. With reduced energy consumption and hydraulic losses, it supports sustainability goals and environmental benefits, making it a versatile solution for various industries.

Acknowledgements

This work is supported by MET's Institute of Engineering, Nashik, and Savitribai Phule Pune University, India, as well as Indo Pump India Limited, Ambad, Nashik.

Nomenclature

g – acceleration m/s^2
H – total head, m
P – pressure at a point, N/m^2
ΔP – differential pressure, kg/cm^2
Q – discharge, m^3/s
v – velocity of fluid, m/s
z – elevation head, m
α – correction factor
η – efficiency of pump
ρ – density of fluid, kg/m^3

References

[1] Liu H., Cheng Z., Ge Z., Dong L. and Dai C. (2021): *Collaborative improvement of efficiency and noise of bionic vane centrifugal pump based on multi-objective optimization.*– Advances in Mechanical Engineering, vol.13, No.2, pp.1-15, DOI: 10.1177/1687814021994976.

[2] Euyoqui Aréchiga F.J., Suástegui Macías J.A., Bonilla D., Acuña Ramírez A., Pérez Sánchez A. and Magaña Almaguer H.D. (2024): *Evaluation of energy efficiency actions in Mexican aqueducts with an approach on their performance over time.*– Heliyon, vol.10, No.e40594, pp.1-17, DOI: 10.1016/j.heliyon. 2024.e40594.

[3] Zhang Y. and Song C. (2023): *A novel design of centrifugal pump impeller for hydropower station management based on multi-objective inverse optimization.*– Processes, vol.11, No.3335, pp.1-20, DOI: 10.3390/pr11123335.

[4] Jiang Q., Heng Y., Liu X., Zhang W., Bois G. and Si Q. (2019): *A review of design considerations of centrifugal pump capability for handling inlet gas-liquid two-phase flows.*– Energies, vol.12, No.1078, pp.1-18, DOI: 10.3390/en12061078.

[5] Cao P., Wang Y., Kang C., Li G. and Zhang X. (2017): *Investigation of the role of non-uniform suction flow in the performance of water-jet pump.*– Ocean Engineering, vol.140, pp.258-269. DOI: 10.1016/j.oceaneng.2017.05.031.

[6] Dai C., Guo C., Chen Y., Dong L. and Liu H. (2021): *Analysis of the influence of different bionic structures on the noise reduction performance of the centrifugal pump.*– Advances in Mechanical Engineering, vol.21, No.3, pp.886-895, DOI: 10.3390/s21030886.

[7] Liu J., Zhang F., Zhu L.F., Yuan S.Q., Xu R.H. and Zhang H. (2024): *Influence of bionic structure on hydraulic performance and drag reduction effect of a centrifugal pump.*– Journal of Physics: Conference Series, vol.2707, No.1, pp.012044-012052, DOI: 10.1088/1742-6596/2707/1/012044.

[8] Hijazi S. and Tolouei E. (2024): *Bio-inspired surface texture fluid drag reduction using large eddy simulation.*– Journal of Applied Fluid Mechanics, vol.16, No.6, pp.1175-1192, DOI: 10.47176/jafm.16.06.1502.

[9] Graybill M.T. and Xu N. (2024): *Experimental studies of bioinspired shark denticles for drag reduction.*– Integrative and Comparative Biology, vol.64, No.3, pp.742-752. DOI: 10.1093/icb/icae086.

[10] Mohammadikarachi A., Yousif M., Song J. and Lim, H. (2024): *Exploring near-wake structures: Bio-inspired C-D riblets on circular bluff bodies.*– Journal of Fluids Engineering, vol.147, No.1, pp.1-11, DOI: 10.1115/1.4066113.

[11] Xiao G., Zhang Y., He Y. and He S. (2020): *Optimization of belt grinding step over for biomimetic micro-riblets surface on titanium alloy blades.*– The International Journal of Advanced Manufacturing Technology, vol.110, No.1, pp.1503-1513, DOI: 10.1007/s00170-020-05935-1.

[12] Gabler-Smith M.K. and Lauder G.V. (2022): *Ridges and riblets: Shark skin surfaces versus biomimetic models.*– Frontiers in Marine Science, vol.9, No.1, pp.1-8, DOI: 10.3389/fmars.2022.975062.

[13] Fan S., Han X., Tang Y., Wang Y. and Kong X. (2022): *Shark skin–An inspiration for the development of a novel and simple biomimetic turbulent drag reduction topology.*– Sustainability, vol.14, No.24, pp.1-20, DOI: 10.3390/su142416662.

[14] Ibrahim M.D., Amran S.N.A., Zulkharnain A. and Sunami Y. (2018): *Streamlined vessels for speedboats: Macro modifications of shark skin design applications.*– AIP Conference Proceedings, vol.1929, No.1, pp.1-6, DOI: 10.1063/1.5021936.

[15] Yang K., Yu X., Cui X., Chen D., Shen T., Liu Z., Zhang B., Chen H., Fang R., Dong Z. and Jiang L. (2025): *Surface modification of 3D biomimetic shark denticle structures for drag reduction.*– Advances in Materials, vol.1, No.1, pp.1-10, DOI: 10.1002/adma.202417337.

[16] Dean B. and Bhushan B. (2010): *Shark-skin surfaces for fluid-drag reduction in turbulent flow: A review.*– Philosophical Transactions of the Royal Society A: Mathematical, Physical and Engineering Sciences, vol.368, No.1929, pp.4775-4806, DOI: 10.1098/rsta.2010.0201.

[17] Wang Y., Dong L., Zhou R., Guo C. and Dai C. (2024): *Energy loss and noise reduction of centrifugal pump based on bionic V-groove geometry.*– Water, vol.16, No.15, pp.2183-2195, DOI: 10.3390/w16152183.

[18] Zhang H., Tang L. and Zhao Y. (2020): *Influence of blade profiles on plastic centrifugal pump performance.*– Advances in Materials Science and Engineering, vol.2020, No.1, pp.1-15, DOI: 10.1155/2020/6665520.

[19] Barmaki R. and Ehghaghi M.B. (2019): *Experimental investigation of a centrifugal pump hydraulic performance in hydraulic transmission of solids.*– Mechanics and Mechanical Engineering, vol.23, No.1, pp.259-270, DOI: 10.2478/mme-2019-0035.

[20] Singh K., Singh A. and Singh D.K. (2025): *Modelling and optimization of fluid frictional torque in a single-stage centrifugal pump with a vaned diffuser based on RSM, ANN, and desirability function.*– Journal of Applied Fluid Mechanics, vol.18, No.3, pp.728-741, DOI: 10.47176/jafm.18.3.2906.

[21] Hooshmand R.A. and Joorabian M. (2006): *Design and optimisation of electromagnetic flow meter for conductive liquids and its calibration based on neural networks.*– IEE Proceedings - Science, Measurement and Technology, vol.153, No.4, pp.139-146, DOI: 10.1049/ip-smt:20050042.

[22] Kara Omar A., Khaldi A. and Ladouani A. (2017): *Prediction of centrifugal pump performance using energy loss analysis*.– Australian Journal of Mechanical Engineering, vol.15, No.3, pp.210-221, DOI: 10.1080/14484846.2016.1252567.

[23] White F.M. (2015): *Fluid mechanics* (8th ed.).– McGraw-Hill Education.

[24] Karassik I.J., Messina J.P., Cooper P. and Heald C.C. (2008): *Pump handbook* (4th ed.).– McGraw-Hill Education.

[25] Fox R.W., McDonald A.T. and Pritchard P.J. (2011): *Introduction to fluid mechanics* (8th ed.).– John Wiley and Sons.

[26] Gu X., Su G., Sharma S., Voros J.L., Qin Z. and Buehler M.J. (2016): *Three-dimensional printing of bio-inspired composites.*– Journal of Biomechanical Engineering, vol.138, No.2, pp.1-16, DOI: 10.1115/1.4032423.

[27] Deshmukh P.A., Deshmukh K.D. and Mandhare N.A. (2020): *Performance enhancement of centrifugal pump by minimizing casing losses using coating.*– SN Applied Sciences, vol.2, No.2, pp.1-10, DOI: 10.1007/s42452-020-2042-7.

[28] Wen L., Weaver J.C. and Lauder G.V. (2014): *Biomimetic shark skin: Design, fabrication and hydrodynamic function.*– The Journal of Experimental Biology, vol.217, No.9, pp.1656-1666, DOI: 10.1242/jeb.097097.

[29] Cui B., Wang Z., Zhang Y.-B. and Han X. (2022): *Drag and pressure pulsation reduction of a low-specific-speed centrifugal pump by employing bionic structure.*– Modern Physics Letters B, vol.36, No.6, pp.1-12, DOI: 10.1142/s0217984921506119.

[30] Liu J., Zhang F., Zhu L., Yuan S., Xu R. H. and Zhang H. (2024): *Influence of bionic structure on hydraulic performance and drag reduction effect of a centrifugal pump.*– Journal of Physics: Conference Series, vol.2707, No.1, pp.1-18, DOI: 10.1088/1742-6596/2707/1/012044.

Received: February 5, 2025
Revised: July 30, 2025